45th AIAA Aerospace Sciences Meeting and Exhibit
8 - 11 January 2007, Reno, Nevada

AIAA 2007-438

Offset stream technology – comparison of results from UCI and GRC Experiments

K. B. M. Q. Zaman, [1] J. E. Bridges[2]
NASA Glenn Research Center
Cleveland, OH 44135

and

D. Papamoschou[3]
University of California at Irvine
Irvine, CA 92697

Abstract

Experimental results obtained in the UCI and GRC facilities, on noise reduction due to flow deflectors applied in the fan stream of a separate-flow nozzle, are compared. The nozzles involved in the former facility are geometrically similar but about 8 times smaller than those in the latter. In general, there is good agreement in the effect of the deflectors observed in the two facilities. For a bypass ratio 8 nozzle, the changes in the noise spectral characteristics effected by two pairs of vanes are found to be essentially identical. The overall noise attenuation (in terms of effective perceived noise level) is up to 0.4 EPNdB for this nozzle. For a lower bypass ratio nozzle, on the other hand, significantly more attenuation is observed, however, the attenuation in the GRC facility (1.8 EPNdB) is not as pronounced as observed in the UCI facility (3.1 EPNdB). Possible reasons for the discrepancy are discussed.

1. Introduction

Significant noise reduction had been demonstrated in past experiments at the University of California at Irvine (UCI) for coannular jets with the 'offset stream' concept.[1,2] The concept involves diverting the outer annular stream to one side with respect to the primary stream. When this is done, less noise is heard on the thicker annular side relative to the noise of the concentric case. A small-scale model of a bypass ratio 5 nozzle (referred to as '3BB'), used earlier at the Glenn Research Center (GRC) for studying the effect of chevrons,[3] was employed in the UCI study. Various methods, including placement of vanes and wedges in the outer passage, were tried to offset the outer stream and the resultant effect on the radiated noise was investigated. The efforts produced promising noise reductions.[4] These developments prompted a large-scale test in the Aeroacoustic Propulsion Labora-

[1] Aerospace Engineer, Inlet & Nozzle Branch, Propulsion Systems Division, AIAA Associate Fellow.
[2] Aerospace Engineer, Acoustics Branch, Propulsion Systems Division, AIAA Associate Fellow.
[3] Professor, Department of Mechanical and Aerospace Engineering, AIAA Associate Fellow.

tory (AAPL, also referred to as the 'Dome') at GRC. The objective was to verify and further investigate the noise reduction in nozzles with realistic engine exhaust conditions.

The GRC experiment was completed in late 2005. A large segment of the effort was devoted to a parametric study of the noise reduction with a bypass ratio of 8 nozzle (referred to as '5BB').[5] In order to compare with the UCI results, data were also obtained for the 3BB nozzle. Geometrically similar wedge and vane configurations were tested to compare with the results obtained earlier at UCI. Limited results of the wedge effect were included in Ref. 6. While a 'design of experiments' matrix was followed in the GRC experiment to optimize the vane configuration with the 5BB nozzle,[5] the configurations tested for the 3BB case were not the result of optimization. The objective of the present paper is to document and discuss the comparative results for the 3BB as well as the 5BB nozzles. The aim is to identify conditions under which there was agreement with the UCI data, conditions under which there was disagreement, and provide an analysis and discussion.

2. Experimental Procedures

A photograph of the 3BB nozzle used in the GRC experiment is shown in Fig. 1(a). The corresponding small-scale nozzle used in the UCI experiment is shown in Fig. 1(b). The latter was fabricated by stereo-lithography technique. The two nozzles are geometrically similar except for the nozzle lip and some of the wall thicknesses that are relatively larger in the UCI case because of the small size. The GRC nozzle with 'fan diameter', D_f = 24.46 cm, is about 8 times larger than the UCI nozzle (Table 1). The data shown in this paper pertain to a 'take-off condition' with pressure and temperature ratios (NPR and NTR, respectively) as listed in Table 2. While the pressure ratios were the same in the UCI experiment as in the GRC case, the temperature effect (i.e., density effect) was simulated by helium-air mixture. Figure 2 shows a schematic of the nozzle fitted with vanes and a wedge. Also shown in this figure are the definitions of the polar angle (θ) and the azimuthal angle (ϕ) for the location of the microphone measuring the far-field noise. The notation ϕ is also used for the azimuthal location of the vanes within the fan stream. For the vanes case, two pairs are employed. The upper pair is positioned at ϕ_1 = 110°, and the lower pair at ϕ_2 = 70°, relative to the bottom-dead-center. The angles-of-attack of the upper and lower pairs are denoted by α_1 and α_2, respectively. NACA0012 airfoil shapes, with chord lengths of 3.35 cm, are employed in the GRC experiments. The vanes were simply flat plates with rounded leading edge in the UCI case. The wedge considered in this study is 'internal', filling the annular passage with its base located at the fan nozzle exit. It has an 11 degree half-angle. The microphone location and other pertinent parameters for noise measurement are listed in Table 1.

3. Results and Discussion

Figure 3 compares sound pressure level spectra from the two facilities for both the 3BB and the 5BB nozzles. These data are for the 'baseline' case, (denoted 'Bsln' in the figure legends), without the application of any flow deflection device. The data shown are corrected for atmospheric attenuation.[7] All data are reduced and referenced to the GRC fan diameter and 0.3048-meter distance. The r.m.s. pressure fluctuation, p', within a bandwidth Δf scales as,[8] $(p'/\rho_j U_j^2)^2 (r/D)^2 (U_j/(\Delta f D))$; thus, with the same jet velocities, the UCI data are converted as,

$$SPL_1 = SPL_2 + 20\log_{10}\left(\frac{r_2 D_1}{r_1 D_2}\right) - 10\log_{10}\left(\frac{D_2 \Delta f_2}{D_1 \Delta f_1}\right).$$

Here, r is the distance of the microphone from the nozzle, D is the diameter of the nozzle and subscripts '1' and '2' pertain to GRC and UCI facilities, respectively.

The sets of data in Fig. 3 are for the polar location, θ=30°. The upper pair of curves is for the 3BB nozzle. (The amplitudes are larger since it involves a lower bypass ratio. The core nozzle diameter is larger with this nozzle (Table 2); thus the mass flow rate for the high-speed core flow is larger yielding more noise.) It can be seen that despite a large difference in the nozzle sizes the overall agreement between data from the two facilities is good. The peak amplitudes are within 1.5 dB and the general spectral shapes agree well. However, there are differences, especially on the high frequency end. The UCI data for the 3BB case exhibit higher noise in the frequency range of 1-10 kHz. This affects the prediction for scaled-up effective perceived noise levels (EPNL), as discussed further in the text. Comparatively, the agreement between the two facilities for the 5BB case is excellent. The two curves are practically identical on the high frequency end. Similar comparison at θ=90° show good agreement on the high frequency end for both nozzles. However, the 5BB case exhibits higher noise on the low frequency end, as further discussed later.

Except for the UCI 3BB case, the spectral traces in Fig. 3 exhibit a change of slope around 5kHz. Figure 4 examines if 'rig noise' contributed to this for the GRC data. The jet noise spectrum, as measured, is compared in this figure with the rig noise spectrum. The latter is obtained by taking the nozzle off while maintaining approximately the same mass flow rate. The 'free jet' exit through which the flow exhausted had an area 2.7 times larger than the fan nozzle area; thus the velocity for the rig noise case was smaller by approximately the same factor. It can be seen that the rig noise is at least 10dB lower up to about 10 kHz. Thus, the change in slope around 5kHz, noticeable also in the raw spectrum (solid curve, Fig. 4), appears to be real and not due to rig noise. Note that the jet noise amplitudes are lower than the rig noise at high frequencies apparently because the nozzle cuts off the transmission of high frequency internal noise. Note furthermore that there is a sharp drop-off in the amplitudes at high frequencies due to atmospheric attenuation. This is corrected for in the spectra shown in Fig. 3 as well as all spectral data shown in the following. (It should be noted that for some of the cases in the GRC experiment the spectra contained a tone at about 3 kHz due to flow over a screw-hole. The source was clear since the tone went away when the hole was covered with adhesive tape. However, because of the hot core flow conditions, the hole had to be left uncovered for the rest of the experiment. It was determined that the tone had negligible effect on the spectral shapes as well as on the calculated EPNdB values. This is to be discussed further in Ref. 9. In the present paper the tone has been simply taken out from the spectra for clarity using a suitable algorithm.)

The effect of the wedge on the 3BB nozzle, observed in the two facilities, is now compared in Figs. 5-7. Sound pressure level spectra at θ = 30° are shown in Fig. 5. Data for two azimuthal measurement locations (ϕ, Fig. 2) are compared with the baseline data. Upper and lower figures are for the UCI and GRC cases, respectively. A similar noise reduction is observed in both facilities, for both 'flyover' (ϕ=0°) and 'sideline' (ϕ=60°) locations. The amplitude reduction is somewhat less in the GRC facility; for f > 4 kHz the amplitudes are practically identical with or without the wedge. At

θ=90° (Fig. 6) the comparison is not favorable; the wedge has resulted in significantly higher noise in the GRC facility. These trends are reflected in the directivity plots (overall sound pressure level versus θ) shown in Fig. 7. Noise reduction is achieved by the wedge over most of the polar locations in the UCI facility. There is a 'cross-over' in the amplitudes at $\theta \approx 100°$ with slightly higher noise at yet larger θ. In comparison, the crossover occurs at $\theta \approx 70°$ in the GRC experiment and noise is significantly higher at large θ. At small θ, however, the amplitudes agree quite well between the two facilities. Also indicated in the legend of the directivity plots are the EPNL values calculated from the spectral data. In the calculation, a flight Mach number of 0.28 is invoked at a flyover height of 457 meters with a scale-up factor of 7.8. The data indicate a reduction by 3.9 EPNdB in the UCI facility whereas by only 0.8 EPNdB in the GRC facility.

Figure 8 compares spectral data for the 3BB nozzle with and without 4 vanes, at θ =30°, in a similar manner as in Fig. 5. The vane configuration in this case, denoted as '4V' in the legend, involves two pairs located at the azimuthal locations (ϕ) of 70° and 110°. The upper and lower pairs have angles-of-attack of 10° and 15°, respectively. The graph on the top compares the vane effect for the UCI experiment. Corresponding result for the GRC experiment is shown in the lower graph. For the vane cases, the microphone location is at ϕ=0°, on the side where the annular stream is diverted. It is found that the overall trend for the vane effect is quite similar in the two experiments. However, as with the wedge, the amplitude reduction is somewhat less in the GRC facility. The amplitudes are almost identical for f>7kHz in the GRC experiment whereas the reduction persists up to the highest frequency covered in the UCI experiment. Corresponding spectral data for the polar location θ =90° (microphone at ϕ=0°) are shown in Fig. 9. Here, the vanes have produced somewhat higher noise levels, relative to the baseline case, and the effect is essentially identical in both facilities.

Figure 10 presents the directivity plots with and without the vanes. It can be seen that the noise reduction is pronounced at shallow polar locations. There, the reduction is somewhat less in the GRC case. With increasing θ, as in the wedge case, there is a cross-over in the amplitudes and the noise is higher with the vanes. The crossover location is at $\theta \approx 60°$ in the GRC case as opposed to $\theta \approx 75°$ in the UCI case. The UCI data exhibit a reduction of 3.1 EPNdB. The corresponding reduction for the GRC data is 1.8 EPNdB.

The effect of a vane configuration for the 5BB nozzle is similarly presented in Figs. 11, 12 and13. In the GRC experiment detailed data were obtained for the effect of two pairs of vanes following a 'design of experiments' (DOE) matrix, with angle-of-attack (α), azimuthal location (ϕ) and axial location (x) of the vanes being variables. Three configurations from this matrix were also investigated at UCI. Whereas the 3BB case results, obtained earlier at UCI, prompted the GRC experiment, the UCI data with the 5BB nozzle were obtained after the GRC experiment. This was done in an effort to further explore facility dependence of the results. The angles-of-attack of the vanes for the 5BB case together with those for the 3BB '4V' case are listed in Table 3. The data shown in Fig. 11-13 are for the '4V #3' case. In Fig. 11, once again, the effect of the vanes is similar in the two facilities with less pronounced effect on the high frequency end in the GRC case. The relative effects at θ =90° (Fig. 12) agree quite well. Referring back to the discussion of Fig. 3, note that the UCI data at this polar location exhibit higher noise with symptoms of reflections on the low frequency end. However, in the EPNL calculation the difference at the low frequencies does not weigh in. The directivity data compared in Fig. 13 exhibit good agreements between the two facilities. Note, however, that the vanes have produced little or no reduction in the EPNL in either facility (0.3 EPNdB for UCI and 0 for GRC). The best vane case from the DOE matrix in the GRC (5BB) experiment yielded 0.4 EPNdB reduction.[5]

As listed in Table 3, three vane cases with the 5BB nozzle were investigated at UCI. The directivity plots for the 3 cases are shown in Fig. 14. Corresponding GRC results are shown in Fig. 15. For these GRC data, the trailing edge of the vane (with $\alpha=0$) was located at 0.5 chord upstream from the fan nozzle exit. This was approximately the case in the UCI experiment. The data for vane case #3 show an increase in the amplitudes at large polar angles in the GRC experiment. However, the trends seen in Figs 14 and 15, particularly at shallow angles, are in excellent agreement between the two facilities. Considering the fact that noise measurements are often sensitive to small differences in the facility conditions, the agreement in the trends with varying angles-of-attack is quite remarkable. Note from the numbers in the legend that while the observed effects match very well, reductions in EPNL range only up to 0.4 dB (GRC case #2).

Flight effect on the noise reduction by the vanes is shown in Figs. 16 and 17, with data from the GRC experiment. While the flight effect is simulated with a free jet in the GRC facility, all UCI results are for zero flight Mach number. In Fig. 16 directivity data for the 4V case with the 3BB nozzle are presented. The curves with the solid data points are with flight Mach number, $M_i = 0.2$. For easy comparison, corresponding 'static' case data from Fig. 10 are reproduced in this figure (open data points). It can be seen that the trends in the noise reduction are the same with or without flight. However, the amplitudes with flight are significantly lower. With flight, the relative increase in the amplitudes at large θ is more and the cross-over location has shifted to lower θ. This manifests in a smaller decrease in EPNL. While the reduction in the static case is 1.8 EPNdB it is only 0.7 EPNdB with flight. Figure 17 shows the flight effect on the vane cases of Fig. 15. A similar observation can be made as with Fig. 16.

Thus, the noise reduction observed with the flow deflectors appears to diminish with flight. It is also clear that the effect of the flow deflectors is more pronounced when the bypass ratio is lower (significant effect with 3BB but small effect with 5BB). It can be reasoned that with increasing bypass ratio, the effect of the deflectors ought to diminish. Since the fan flow is deflected on the observer side, ideally the least noise achievable should approach that of the fan stream alone (with core flow completely silenced). With high bypass ratio, the noise from the core flow is relatively less. Thus, the amount that can be attenuated is less to begin with. (In the limit of infinite bypass ratio, with zero core flow, the noise is solely from the fan stream and simply shifting it with the deflectors should not make a difference in the noise.) This is borne out by further data obtained in the GRC experiment with a bypass ratio13 case. There is a systematic reduction in the effect with increasing bypass ratio from 5 to 8 to 13. The GRC experiment covered many more cases. In addition to the DOE matrix with the vanes for the 5BB nozzle, wedges of different geometry, different internal plug configuration as well as a case of non-concentric fan nozzle, all with and without flight, were investigated. Further results will be presented in a future paper.[9]

The results obtained for the 3BB nozzle in the UCI and the GRC facilities differed in the amount of noise reduction. The reductions observed at GRC were less. Recall, for example, with the '4V' case (Fig. 10) the GRC data showed 1.8 EPNdB reduction as opposed to 3.1 at UCI. The discrepancy with the 3BB case is thought to be partially due to differences in the baseline data that were somewhat noisier in the UCI experiment. Referring back to Fig. 3, recall that the (UCI) amplitudes were larger in the frequency range of 1-10 kHz. When scaled up for EPNL calculations, these higher amplitudes weigh in. Figure 18 further explores the sources of the difference. 'Noy' spectra (spectra filtered to account for human perception, leading to EPNL calculation) are compared between the two facilities. Data are shown for four polar locations. The comparisons agree well for the larger polar locations (72° and 91°). However, the reduction in the amplitudes in the UCI case is more at the two smaller polar locations (30° and 52°). From similar plots at several more locations it is inferred that that the difference in the EPNL values is contributed to mostly from data in the θ-range of 30°-60°. Note that the amplitudes with the vanes (blue dotted curves) are relatively comparable between the two facilities. The amplitudes for the baseline case (red solid curves) are larger in the UCI case. This manifested in a larger noise reduction in the UCI experiment.

Why is the 3BB baseline case noisier in the UCI facility? It is conjectured to be due to differences in the detailed geometries of the nozzles in the two experiments. The UCI 3BB nozzle was fabricated about 3 years ago when the fidelity in the stereo-lithography process employed there was not as good as today. For example, because of the small dimensions, the relative thickness of the nozzle lip was larger than that in the GRC nozzle. The core nozzle lip-thickness to fan-diameter ratio in the GRC cases is 0.0033 while that in the UCI 3BB case is 0.025. The UCI 5BB nozzle, on the other hand, was fabricated later when the fabrication process improved. The lip-thickness to fan-diameter ratio was reduced to 0.013. Also, the contours (flow lines) of the nozzles for the 5BB case were replicated with better fidelity. As a result, even though the noise reduction is not much, the comparative effects observed at the two facilities for the 5BB nozzle are more favorable. This is further illustrated with the Noy spectra in Fig. 19, presented in a similar manner as in Fig. 18.

4. Concluding Remarks:

Experimental results obtained in UCI and GRC facilities, on noise reduction due to flow deflectors, have been compared. The nozzles involved in the latter facility are geometrically similar but roughly 8 times larger than those in the former. Results are presented for two different nozzle configurations having bypass ratio of 5 (3BB) and 8 (5BB). The vanes did not produce significant noise reduction with the 5BB nozzle in either facility. Both vanes and a wedge produced significant noise reduction for the 3BB nozzle. The reduction in spectral amplitudes was similar at shallow angles, in either facility. However, the GRC data showed little effect at high frequencies. Also, at locations perpendicular to the jet axis the comparison was poor for the wedge case. There, the spectral amplitudes were significantly larger with the wedge in the GRC case. Thus, in EPNL scale whereas the UCI data yielded a reduction by 3.9 EPNdB, the GRC results showed a reduction of only 0.8 EPNdB. A better comparison was noted for the effect of two pairs of vanes with the 3BB nozzle. The GRC data showed 1.8 EPNdB reduction as opposed to 3.1 at UCI. The discrepancy with the 3BB case is thought to be due to differences in the baseline data that were somewhat noisier in the UCI experiment. The higher noise is thought to be due to differences in the detailed geometry of the nozzle. The UCI 3BB nozzle was fabricated several years ago when the method of fabrication employed did not replicate the nozzle accurately. The 5BB nozzle, on the other hand, was fabricated recently with improved technique. The effects of the vanes were studied for this nozzle and found to be very similar in the two facilities. Thus, even though the overall noise attenuation was not as much as with the 3BB case, the trends in the spectral changes due to the flow deflectors were found to be essentially identical in the two facilities. These results provide reassurance that small scale experiments, with sufficient care, can be valid and useful in jet noise studies. The results presented in this paper also support the validity of significant noise reduction with flow deflectors for moderate- or low-bypass ratio nozzles.

Acknowledgement

Support from the Quiet Aircraft Technology Program and the Subsonic Fixed Wing Program are gratefully acknowledged.

References

[1] D. Papamoschou and M. Debiasi, "Directional suppression of noise from a high-speed jet", *AIAA J.*, 39(3), pp. 380-387, 2001.

[2] Papamoschou, D., "A New Method for Jet Noise Reduction in Turbofan Engines," AIAA Journal, vol. 42, No. 11, pp. 2245-2253, 2004.

[3] Saiyed, N.H., Mikkelsen, K.L. and Bridges, J.E., "Acoustics and thrust of separate-flow high-bypass-ratio engines", AIAA Journal, vol. 41, No. 3, pp. 372-378, 2003.

[4] D. Papamoschou and K. Nishi, "Turbofan jet noise reduction via deflection of the bypass stream", *AIAA Paper* 2004-00187, 42nd AIAA Aerospace Sciences Meeting, Reno, NV, Jan 5-8, 2004.

[5] Henderson, B., Norum, T. and Bridges, J. E., "An MDOE assessment of nozzle vanes for high bypass ratio jet noise reduction", AIAA Paper 2006-2543, 12th AIAA/CEAS Aeroacoustics Conf. (27th AIAA Aeroacoustics Conf.), Cambridge, MA, May 8-10, 2006.

[6] Zaman, K.B.M.Q. and Papamoschou, D., "Effect of a wedge on coannular jet noise", *AIAA Paper* 2006-0007, 44th AIAA Aerospace Sciences Meeting, Reno, NV, Jan 9-12, 2006.

[7] Bass, H.E., Sutherland, L.C., Zuckerwar, A.J., Blackstock, D.T. and Hester, D.M., "Atmospheric absorption of sound: further developments", *J. Acoust. Soc. Am.*, **97**(1), 1995.

[8] Zaman, K.B.M.Q. and Yu, J.C., "Power spectral density of subsonic jet noise", *J. Sound and Vib.*, **98**, pp. 519-537, 1985.

[9] Brown, C., Bridges, J. and Henderson, B., "Offset stream technology test – summary of results", 13th AIAA/CEAS Aeroacoustics Conference, Rome, Italy, May 21-23, 2007.

	UCI	GRC
D_f (cm)	3.1	24.46
Mic. Location, r (m)	1.07	13.73
r/D_f	34.5	56.1
f-range (kHz)	140	100

Table 1 Nozzle dimensions and pertinent parameters for noise measurement.

Nozzle	Core Dia (cm)	Core NPR	Fan NPR	Core NTR	Fan NTR
3BB	13.16	1.69	1.83	2.79	1.19
5BB	12.37	1.42	1.62	2.79	1.19

Table 2 Operating conditions for the GRC experiment. Internal plug and D_f are the same for the two nozzles.

Case	α_1 (deg.) (upper pair)	α_2 (deg.) (lower pair)
3BB 4V	10	15
5BB 4V#1	5	5
5BB 4V#2	7.5	7.5
5BB 4V#3	10	10

Table 3 Angles-of-attack of the vanes. In all cases, upper and lower pairs of vanes are located at ϕ =110° and 70°, respectively.

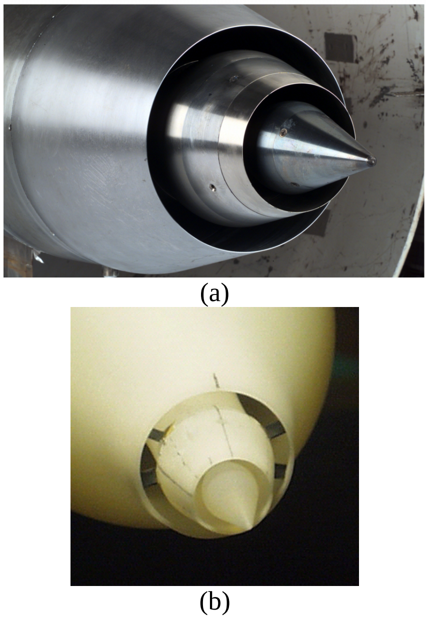

Fig. 1 Pictures of bypass ratio 5 (‘3BB’) nozzle: (a) GRC (D_f = 24.46 cm), (b) UCI (D_f = 3.1 cm).

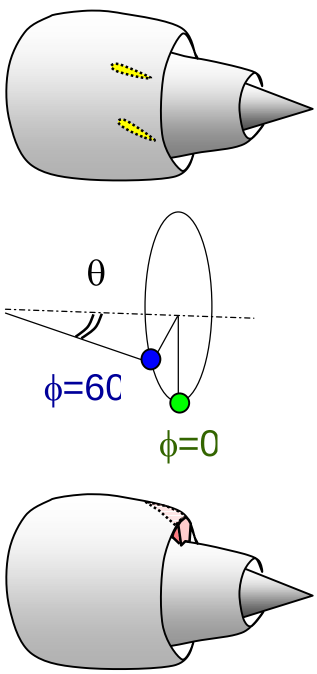

Fig. 2 Schematic of the nozzle with two pairs of vanes (top) and a wedge (bottom) in the fan stream. Reference for polar (θ) and azimuthal (ϕ) measurement locations are shown in the middle sketch.

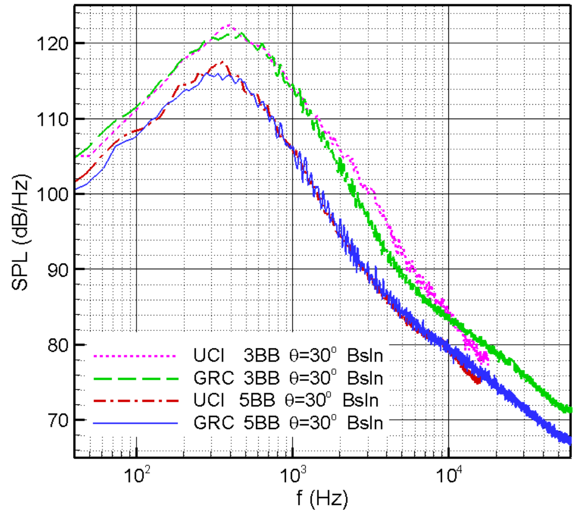

Fig. 3 Comparison of sound pressure level spectra from the two facilities at θ = 30°. All data referenced to GRC fan diameter and 0.3048 m distance.

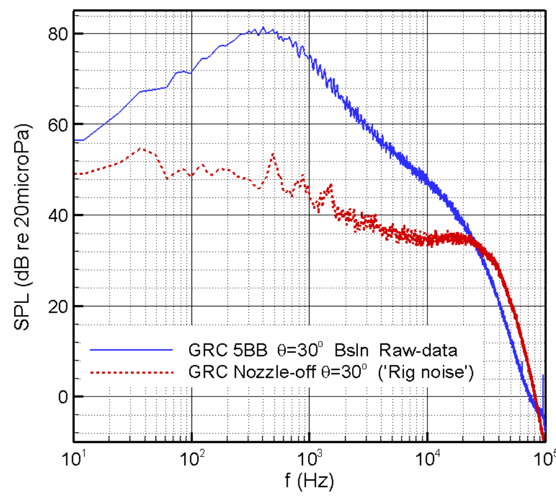

Fig. 4 Raw sound pressure level spectra at θ = 30° for the 5BB nozzle compared to ‘rig noise’ spectra obtained at same flow rate with nozzle taken off .

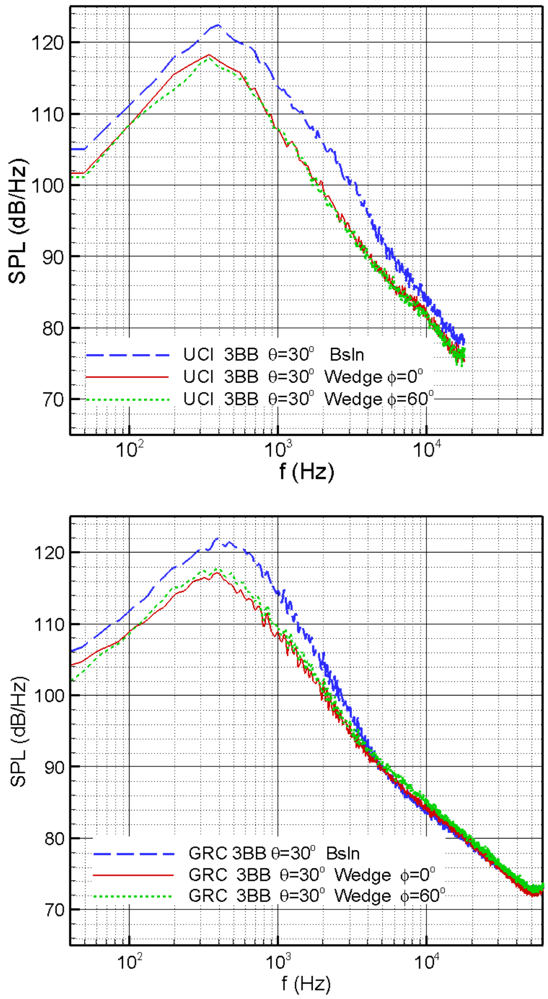

Fig. 5 Sound pressure level spectra showing effect of wedge at $\theta = 30°$ for the 3BB nozzle. Upper figure: UCI data; lower figure: GRC data. Wedges in the two are geometrically similar with 11° half-angle.

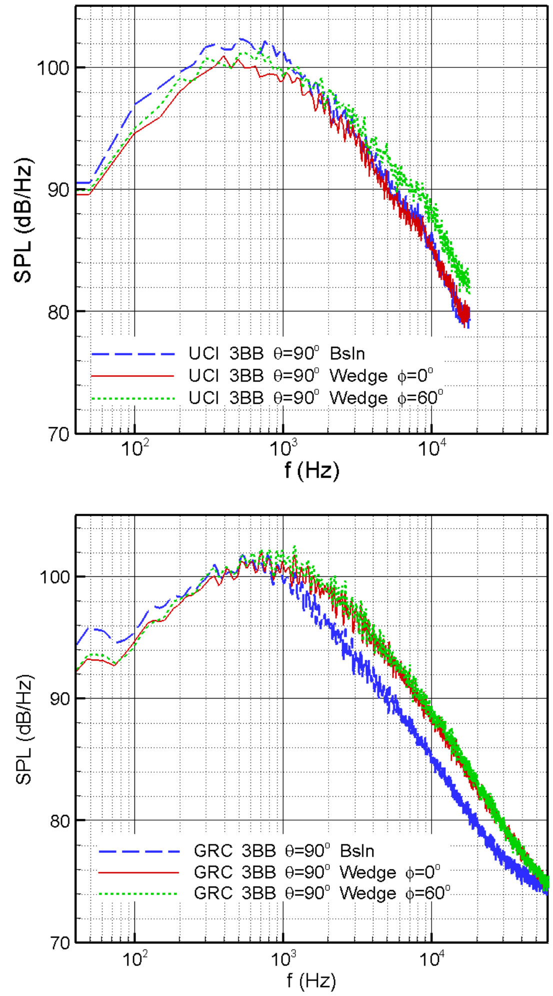

Fig. 6 Data corresponding to Fig. 5 at $\theta = 90°$.

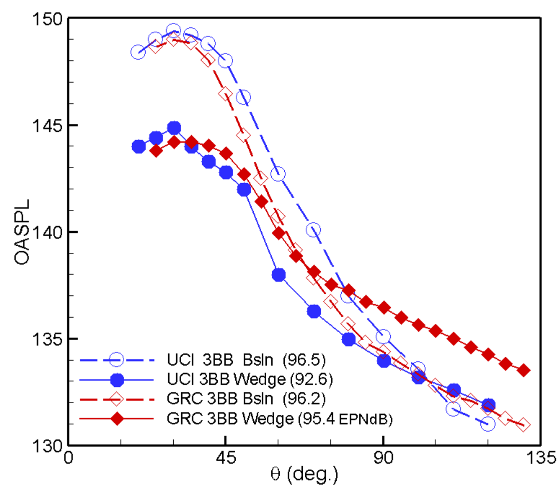

Fig. 7 Overall sound pressure level versus polar angle for the wedge case of Figs. 5 and 6.

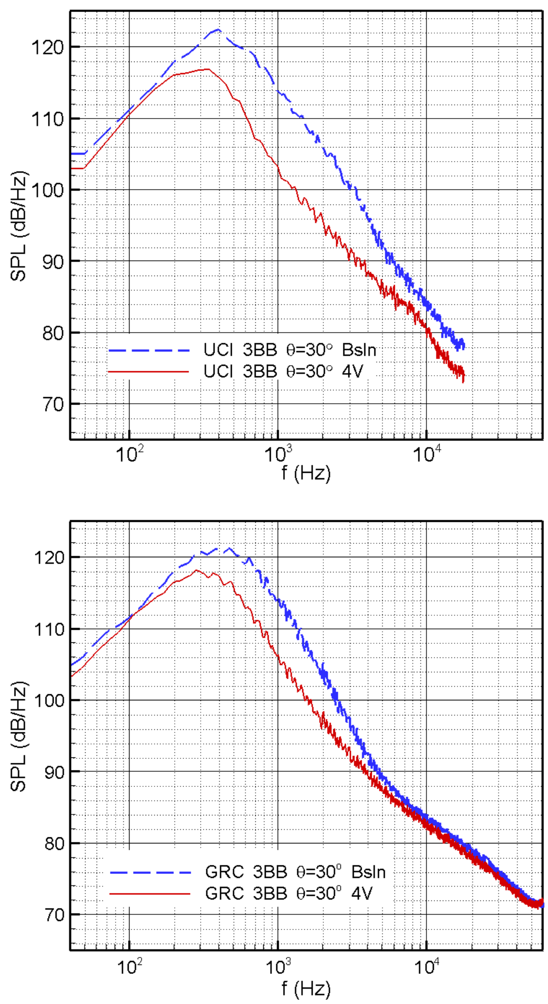

Fig. 8 Sound pressure level spectra showing effect of vanes at $\theta = 30°$ for the 3BB nozzle. The two pairs of vanes are at $\alpha_1 = 10°$ and $\alpha_2 = 15°$. Upper figure: UCI data; lower figure: GRC data.

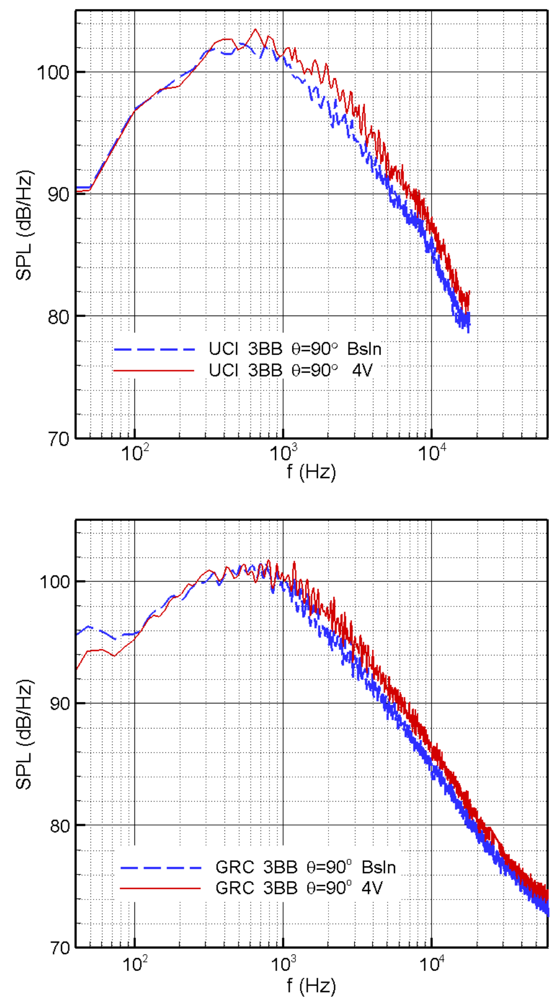

Fig. 9 Sound pressure level spectra corresponding to the conditions of Fig. 8 at $\theta = 90°$.

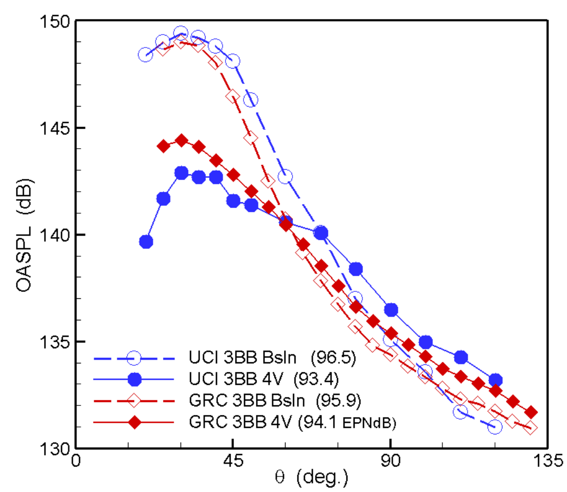

Fig. 10 Overall sound pressure level versus polar angle for the vanes case of Figs. 8 and 9.

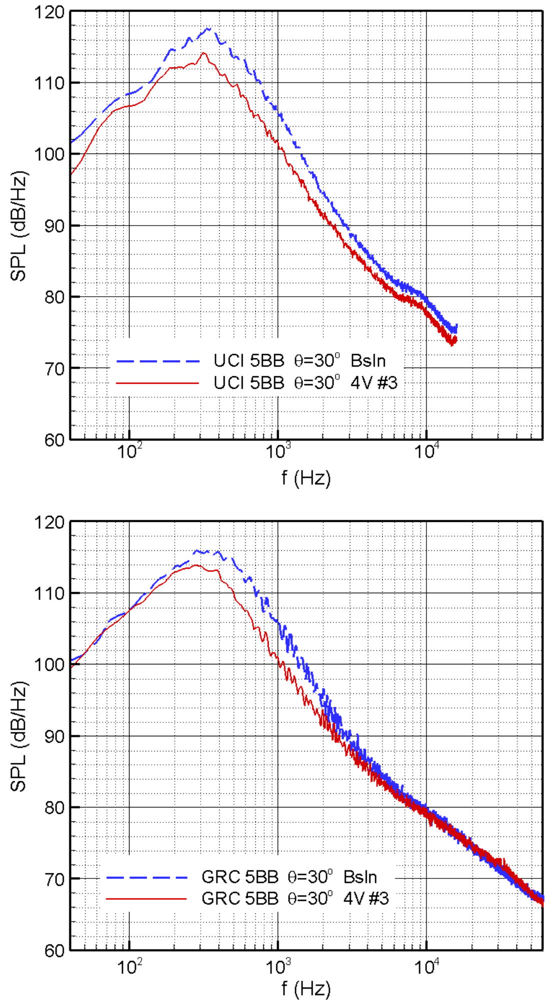

Fig. 11 Sound pressure level spectra showing effect of vanes at $\theta = 30°$ for the 5BB nozzle. The two pairs of vanes are at α_1=10° and α_2=10°. Upper figure: UCI data; lower figure: GRC data.

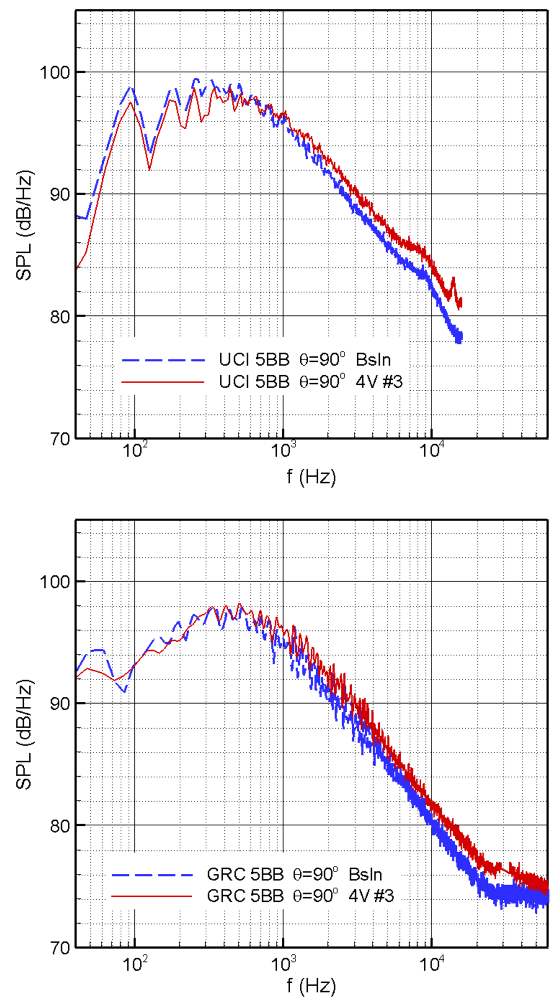

Fig. 12 Sound pressure level spectra corresponding to the conditions of Fig. 11 at $\theta = 90°$.

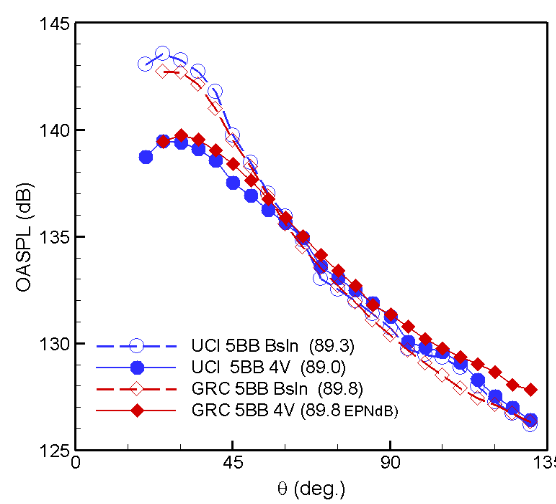

Fig. 13 Overall sound pressure level versus polar angle for the vane cases of Figs. 11 and 12.

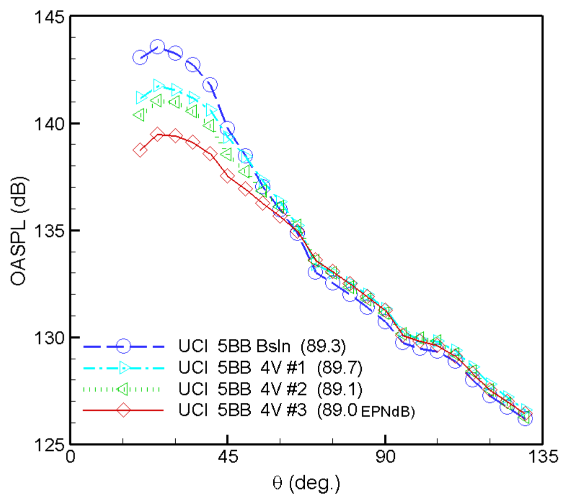

Fig. 14 Overall sound pressure level versus polar angle for 3 vane configurations with the 5BB nozzle; UCI data.

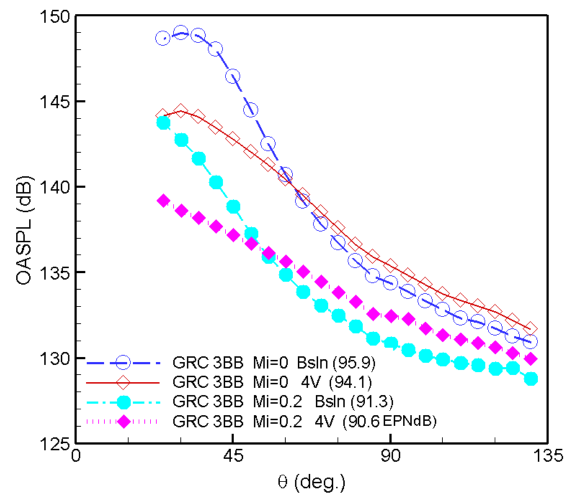

Fig. 16 Overall sound pressure level versus polar angle for the 3BB nozzle with 2 pairs of vanes (α_1=10° and α_2=15°) with flight Mach number, M_i = 0.2. Data for 'static' case from Fig. 10 are reproduced for direct comparison.

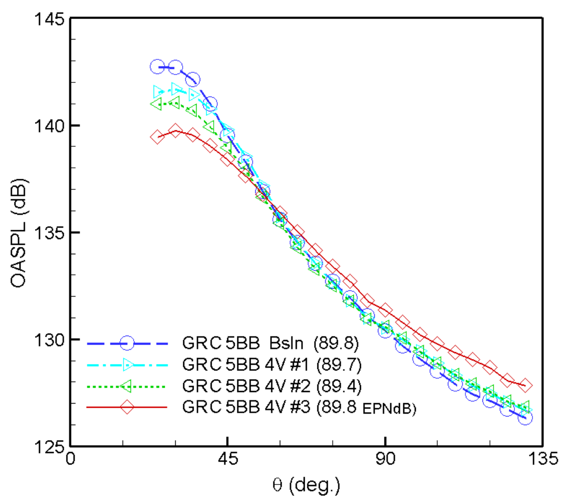

Fig. 15 Overall sound pressure level versus polar angle for 3 vane configurations with the 5BB nozzle; GRC data.

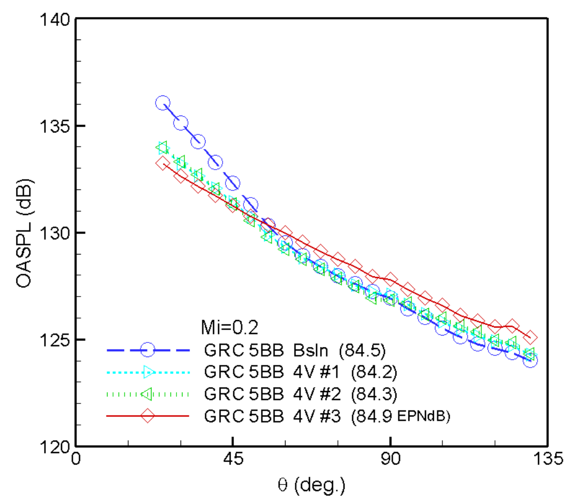

Fig. 17 Overall sound pressure level versus polar angle for the 3 vane configurations of Fig. 15 with flight effect; 5BB nozzle, M_i = 0.2.

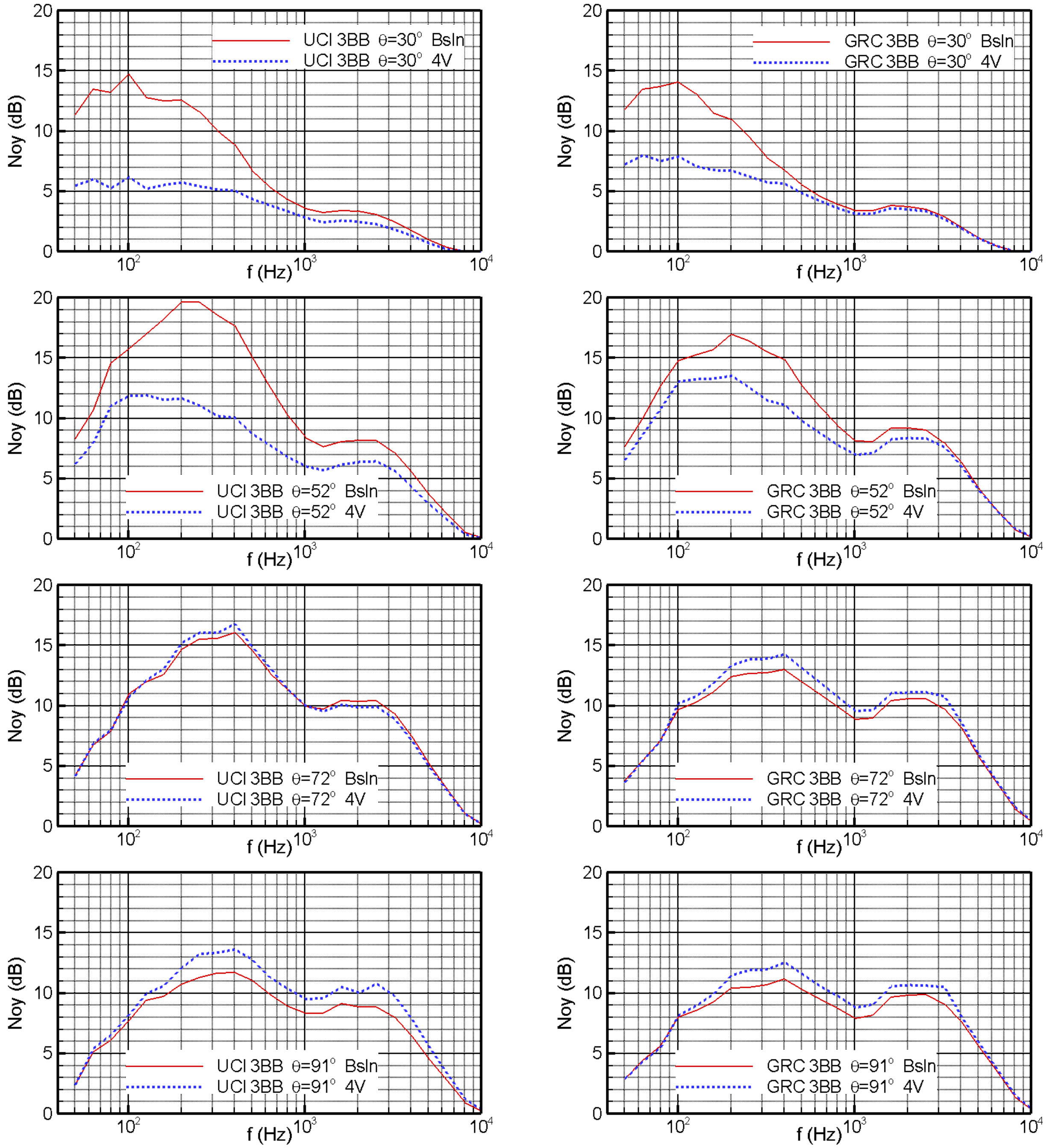

Fig. 18 Comparison of Noy spectra, UCI versus GRC results, for the effect of vanes (4V) with the 3BB nozzle.

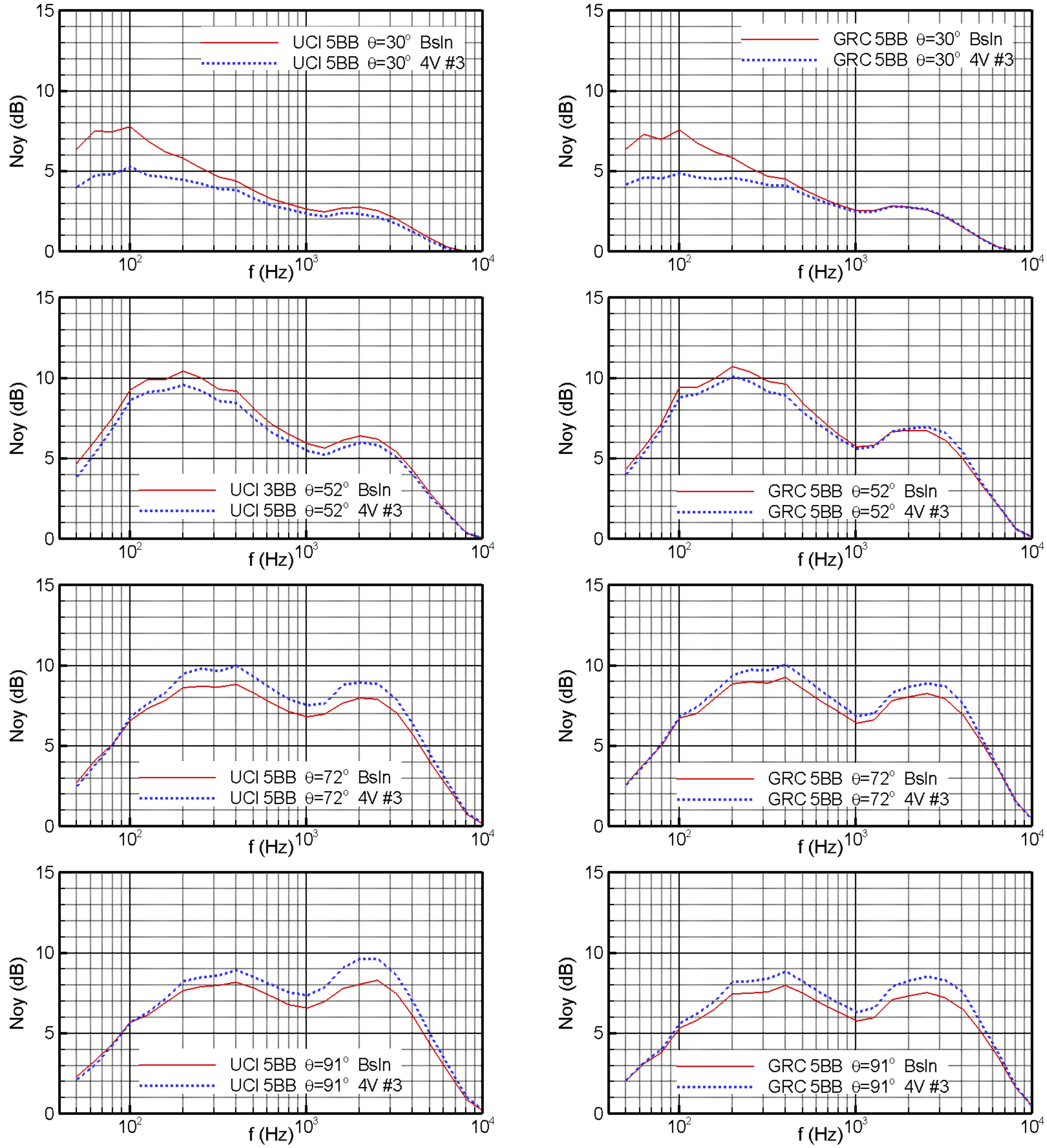

Fig. 19 Comparison of Noy spectra, UCI versus GRC results for the effect of vanes (4V #3) with the 5BB nozzle.